

Supporting Material

Materials and Methods

EAAT5 expression

Molecular biology, transient expression of EAAT5 in HEK293 cells, and electrophysiological recordings of EAAT5 currents were performed as described in detail (1). Briefly, AcGFP-N-terminal-coupled EAAT5 or wildtype EAAT5 expressing cells were either used for electrophysiological, colocalization or L-[³H]-glutamate uptake studies. Fixed cells (4% paraformaldehyde in 10 mM PBS, pH 7.4) were labeled with 5 μg/ml TRICT conjugated Wheat Germ Agglutinin (*Sigma-Aldrich* Deisenhofen, Germany) for 30 min. at room temperature and colocalisation analysis was performed using Wright Cell Imaging Facility ImageJ plugin (2). For immunoblot analysis, aliquots of SDS extracts (10 μg per lane) were subjected to SDS/9% polyacrylamide gel electrophoresis and immunoblotted with EAAT5-specific antibodies (1 μg/ml; BIOTREND Chemikalien GmbH, Köln, Germany). Biotinylated molecular weight markers (Cell Signaling Technology, Frankfurt am Main, Germany) were labeled with Streptavidin conjugated HRP (*Sigma-Aldrich*). Proteins were visualized using ECL (GE Healthcare, München, Germany). L-[³H]-glutamate uptake of membrane vesicle preparations from EAAT5 transfected cells was measured using 1 μCi of L-[³H]-glutamic acid (29 Ci/mmol, GE Healthcare) supplemented with 1 μM unlabelled L-glutamate at a protein concentration of 40 μg (for details: (3)). Experiments were performed in triplicate and all values reported are the mean ± SD of at least three independent observations.

Whole-cell Current Recording

Glutamate-induced currents were measured in the whole-cell current-recording configuration as described with an HEKA series 7 amplifier, under voltage-clamp conditions. The resistance of the recording electrode was 2–3 MΩ; the series resistance, R_s , 4–6 MΩ. SCN^- was used in the intracellular or extracellular solutions because it enhances glutamate transporter-induced currents (4). To determine the anion current induced by SCN^- outflow, the intracellular and extracellular solutions contained 140 mM KSCN, 2 mM $MgCl_2$, 10 mM EGTA, 10 mM HEPES (pH 7.3), and 140 mM NaCl, 2 mM $MgCl_2$, 2 mM $CaCl_2$, 10 mM HEPES (pH 7.3), respectively. For the measurements of anion current induced by anion inflow, external NaCl was substituted by NaSCN and the pipette solution contained KCl. The voltage dependent recordings were done with a fast voltage jump protocol (see corresponding figures for protocol details). In the homoexchange mode experiments the KSCN in the intracellular solution was replaced by 140 mM NaSCN and 10 mM glutamate (saturating concentration) was also added to the intracellular solution.

At steady state, R_s was not compensated because of the small whole-cell currents. In the voltage jump protocol, R_s compensation of 60–80% was used to accelerate the capacitive charging of the membrane in response to the fast jump in voltage.

Modeling

We used two simplified transport models to explain the experimental data (see Scheme 1). The first model is a model that contains the absolute minimum of steps to account for the time and voltage dependent behavior in the anion current in the forward transport mode. The model only contains a slow and voltage dependent, reversible Na^+ binding step to the empty transporter (absence of glutamate), a fast, reversible glutamate binding step, and a slow, voltage dependent and irreversible step that completes the transport cycle (Scheme 1A). Models with Na^+ binding being the only slow step fail to reproduce the experimental data, since they will lead to rapid depletion of anion-conducting states after glutamate binding and, thus, a large overshoot component of the anion current in response to rapid glutamate application. Overshoot components have not been observed experimentally. Therefore, an additional slow step must exist in the transport cycle, which is most likely associated with the Na^+ /glutamate translocation process. In the model in scheme 1A, this slow step is lumped into the overall recycling step connecting states T and NTG. The model predicts the lack of effect of glutamate concentration on the relaxation rate of the slow phase of anion current activation. Assuming that glutamate binding is in fast pre-equilibrium, the slow relaxation rate can be expressed as follows:

$$k_{\text{obs}} = k_1[\text{Na}^+] + \frac{k_{-1}K_d + k_2[\text{Glu}^-]}{K_d + [\text{Glu}^-]} \quad (\text{eq. S1})$$

Here, k_1 and k_{-1} are the rate constant for sodium association/dissociation, k_2 is the rate constant for recycling of the transporter binding sites, and K_d is the dissociation constant of glutamate from its binding site. If the equation is dominated by the rate constant $k_1[\text{Na}^+]$, then k_{obs} becomes independent of glutamate concentration, as found experimentally (Fig. 3D). While this very simplistic model already explains the experimental data very well, it cannot account for the kinetics in the homoexchange mode. Therefore, we extended the model, including additional steps, as shown in Scheme 1B.

The extended model includes the following additional reversible steps: A sodium binding step after glutamate binds and the translocation reaction from an outward facing configuration to an inward facing configuration (characterized by k_t and k_{-t}). We also modeled the step from the $\text{N}_2\text{T}'\text{G}$ (inside) to T' (inside), which is related to the intracellular substrate/ion dissociation steps and is characterized by the rate constants k_i and k_{-i} , and the reverse translocation reaction, from T' into T, characterized by k_r . We assumed this last step to be quasi-irreversible, since we have a high intracellular potassium concentration and an extracellular $[\text{K}^+] = 0$, which drives the reaction into the state T. We also modeled the transport in exchange mode by setting $k_i=0$.

In order to determine the apparent valences associated with the individual transport steps, we took into account the overall charge moved during the transport cycle, according to the known stoichiometry for the other EAAT subtypes, which was assumed as +2, therefore we set $z_{\text{total}} = 2$. Our data show no evidence for any different stoichiometry for EAAT5 from the other transporter subtypes, so this assumption is valid. We assumed the glutamate binding step to be electroneutral, based on the experimental data available for the other glutamate transporter subtypes. We assumed all the other steps, except the intracellular step characterized by the rate constants k_i and k_{-i} , to be electrogenic, with the respective valences obtained after optimization of the program to better describe our experimental data. The valence used for the modeling of the translocation step was $z_Q = 0.6$, which is in agreement with a relatively weak voltage dependence of this step found experimentally for the other members of this family of transporters. The values used in the simulations are displayed in Scheme 1.

The main anion conducting states are TN_2G (outside facing conformation), and $T'N_2G$ (inside facing conformation), with some contribution from the state TN . The reason behind this assumption is that TN_2G is the main conducting state for the other transporters of this family. Our experimental data fits well with postulating both TN_2G and $T'N_2G$ as main anion conducting states. The experimentally measured anion current was considered to be directly proportional to the sum: $(1TN+5TN_2G+7T'N_2G)$.

To determine the voltage dependence of the rate constants (in this example for the forward translocation step) we used the following equation:

$$k_t(V_m) = k_t(0) \exp \frac{(-z_t V_m F)}{2RT} \quad (\text{eq.S2})$$

In this case t refers to the translocation step from the outward facing configuration to the inward facing configuration (see Scheme 1). We used the same equation for all the voltage dependent steps. F is the Faraday constant, T the temperature, R the gas constant.

The voltage dependence of the anion current was calculated using the Goldman-Hodgkin-Katz equation (5-6):

$$I_{SCN} = \frac{P_{SCN} F^2 V_m}{RT} \frac{([SCN^-]_i - [SCN^-]_o \exp(-V_m F/RT))}{1 - \exp(-V_m F/RT)} \quad (\text{eq. S3})$$

P_{SCN} is the channel permeability and F , R and V have the usual meaning.

The kinetic parameters were varied manually, until the simulated results agreed with the experimental curves obtained (Figs. 3B and 4A).

Supporting Figures

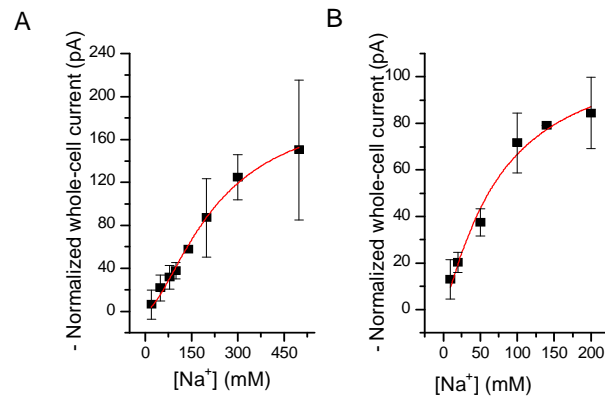


Figure S1. (A) Sodium concentration dependence of EAAT5 anion currents when sodium binds to the empty transporter. The data were recorded in exchange conditions with 10mM glutamate and 140 mM NaSCN applied intracellularly. The unspecific sodium current from non transfected HEK293 cells was subtracted. The data were fitted to the Hill equation with a $K_m = 229 \pm 37$ mM and $n = 1.6 \pm 0.2$ (B) Sodium concentration dependence of sodium binding to the glutamate-loaded transporter. The data were recorded in forward conditions with 140 mM KSCN applied to the inside of the cell, $K_m = 76 \pm 38$ mM.

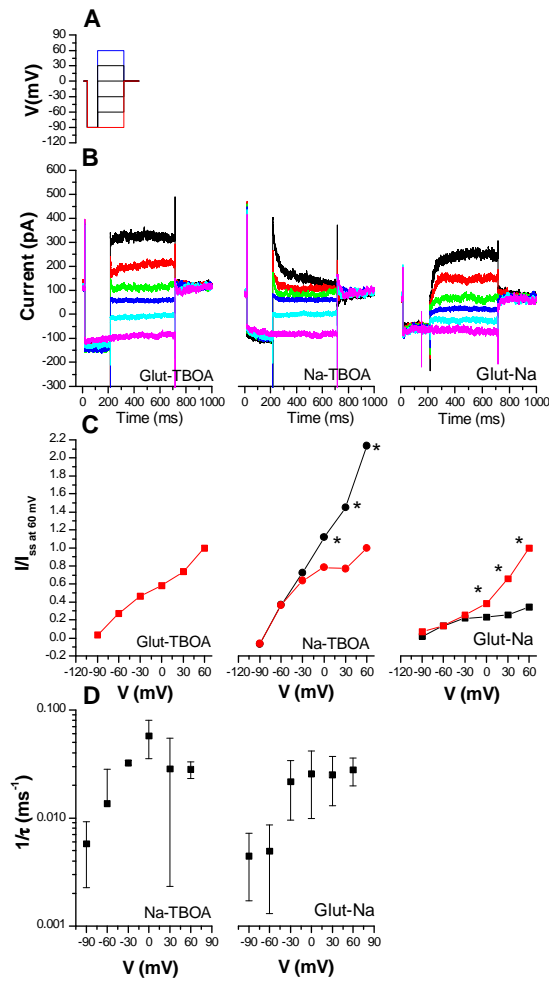


Figure S2. Voltage jump–induced current relaxations in EAAT5, with *SCN* outside (NaSCN) in the applied solutions. (A) Top trace, voltage jump protocol used to measure the current traces shown in B. The protocol starts at 0mV and has a jump to –90 mV then goes to +60mV and then to 0mV as depicted in the figure. The purpose of the initial jump is to increase the amplitude of the observed currents. (B) Typical signals obtained through subtraction of current traces recorded as indicated at the bottom of each picture: (left) subtraction of the traces with glutamate from the traces recorded in the presence of TBOA; (center) subtraction of the traces in the absence of glutamate (extracellular 140mM sodium thiocyanate solution, see methods) from the traces with TBOA; (right) subtraction of the traces in the presence of glutamate (sodium solution as in center) from the traces in the absence of glutamate. (C) Voltage dependence of $I_{initial}$ (black) and I_{SS} (steady state, red) ($I_{initial}$ not observed for the glutamate-TBOA case as can be seen in (B)) currents for each of the plots. The currents are normalized to the observed steady state current at +60 mV, for each of the conditions. The stars denote significance. The glutamate

concentration was $60\mu\text{M}$ (close to the K_m value) and the TBOA concentration was $100\mu\text{M}$ (saturating). (D) Voltage dependence of the additional relaxation component of the anion current, due to a slow relaxation to a new steady state with different open probability, tau values for the voltage induced increase in conductance (relaxation) to a new steady state, with SCN^- outside in the extracellular solution. In the case of Glutamate-TBOA, when SCN^- was applied extracellularly, it was not possible to determine the tau value for the more positive voltages due to the fact that there seems to be no relaxation to a new steady state.

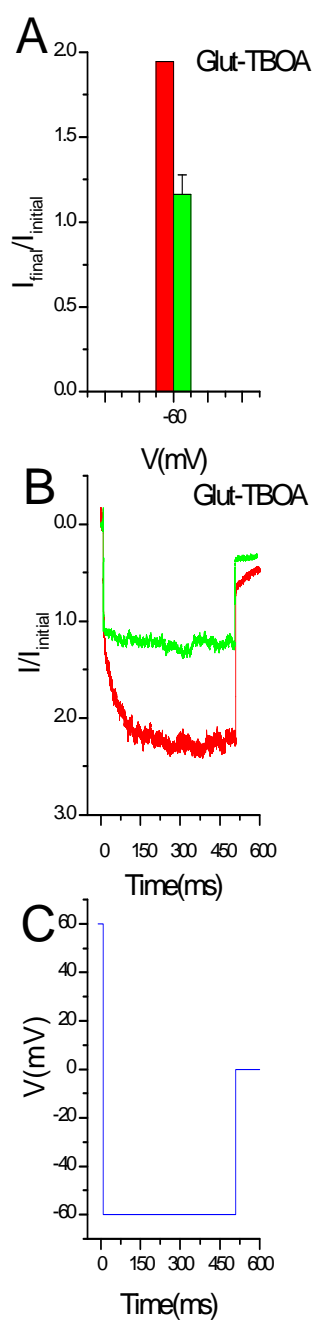


Figure S3. Comparison of the voltage dependence of the additional relaxation component of the anion current (due to a slow relaxation to a new steady state with different open probability) at -60mV , in forward transport mode (red) and in exchange mode (green). The component of the relaxation to a new steady state is much smaller in the case of exchange conditions, where the sodium binding site is saturated (green bar in A and green trace in B). The voltage protocol is in C.

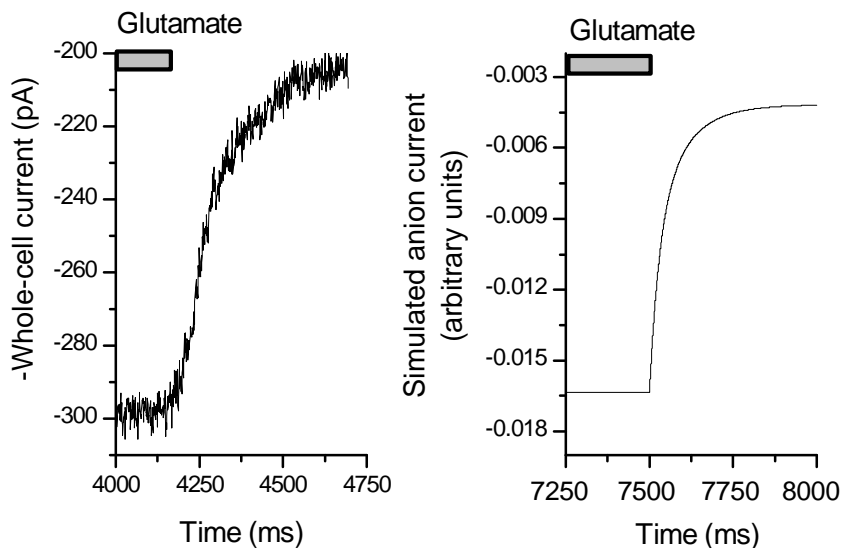


Figure S4. Comparison of the observed and simulated anion current decay, when glutamate was rapidly removed from EAAC1. The concentration of glutamate is $100\mu\text{M}$. The experiments were performed using a fast perfusion system (SF-77B, Warner Instrument Corporation, Hamden, CT), allowing for fast solution changes with a stepper mechanism (solution exchange time for open pipette recording was 5 ms).

References

1. Grewer, C., N. Watzke, M. Wiessner, and T. Rauen. 2000. Glutamate translocation of the neuronal glutamate transporter EAAC1 occurs within milliseconds. *Proc Natl Acad Sci U S A* 97:9706-9711.
2. Manders, E. M. M., F. J. Verbeek, and J. A. Aten. 1993. Measurement of Colocalization of Objects in Dual-Color Confocal Images. *J Microsc-Oxford* 169:375-382.
3. Rauen, T., W. R. Taylor, K. Kuhlbrodt, and M. Wiessner. 1998. High-affinity glutamate transporters in the rat retina: a major role of the glial glutamate transporter GLAST-1 in transmitter clearance. *Cell Tissue Res* 291:19-31.
4. Wadiche, J. I., S. G. Amara, and M. P. Kavanaugh. 1995. Ion fluxes associated with excitatory amino acid transport. *Neuron* 15:721-728.

5. Goldman, D. E. 1943. Potential, Impedance, and Rectification in Membranes. *J Gen Physiol* 27:37-60.
6. Hodgkin, A. L., and B. Katz. 1949. The effect of sodium ions on the electrical activity of giant axon of the squid. *J Physiol* 108:37-77.